# Nano-clay modified multi-walled carbon nanotube composite as a potential adsorbent towards Eriochrome Black T: a comparative study of isotherm and kinetic models

Sabiha Sultana[a,*], Kamran Rehan[b], Imran Rehan[c], Maryelem Churampi Arellano[d], Rand Otbah Farqad[e], Murtadha Laftah Shaghnab[f], Ahmed M. Aljuwayid[g], Saleem Nawaz[a], Rabia Gul[a]

[a]Department of Chemistry, Islamia College University Peshawar, Pakistan 25120, emails: sabiha@icp.edu.pk (S. Sultana), nawazsaleem@myyahoo.com (S. Nawaz), rabiajamal330@gmail.com (R. Gul)
[b]Department of Physics, University of Haripur, Pakistan, email: krehan2010@yahoo.com
[c]Department of Physics, Islamia College University Peshawar, Pakistan 25120, email: irehanyousafzai@gmail.com
[d]Department of Clinical Laboratory, Salutem Centro de Diagnostico, Lima, 150110 Peru, email: Meryelem.cha@gmail.com
[e]Department of Dentistry, Al Noor University College, Nineveh, Iraq, email: rand.otbah@alnoor.edu.iq
[f]College of Pharmacy and Technology, National University of Science, Dhi Qar, Iraq, email: murtadha.laftah.sh@gmail.com
[g]Department of Chemistry, College of Science, King Saud University, P.O. Box: 2455, Riyadh, 11451 Saudi Arabia, email: Aaldossrai@ksu.edu.sa

**ABSTRACT**

Currently environment is endangered by non-biodegradable organic dyes, which has been acknowledged as a serious issue that society must address. In this work, the Eriochrome Black T (EBT) adsorption behavior onto multi-walled carbon nanotube modified montmorillonite (CNT/MMT) composite was examined. Fourier-transform infrared spectroscopy, scanning electron microscopy-energy-dispersive X-ray spectroscopy, thermogravimetric analysis/differential thermal analysis and Brunauer–Emmett–Teller analysis were done before and after adsorption to get insight into adsorption mechanistic by CNT/MMT. Point of zero charge was ascertained to characterize adsorbent surface charge. Batch adsorption studies were performed to apprehend the influence of important adsorption factors namely contact duration, EBT initial concentration, CNT/MMT dosage and adsorption temperature. The EBT adsorption mode and suitability onto CNT/MMT were explored via well-known isotherm models (Langmuir and Freundlich, Dubinin–Radushkevich and Temkin) and kinetic models such as pseudo-first and pseudo-second-order. At 30°C with initial EBT concentration of 25 ppm, adsorbent dosage of 0.5 g, and shaking times of 30 min the maximum removal of EBT by CNT/MMT was found to be 82% (2.1 mg/g), confirming maximum adsorption at low EBT onto heterogeneous surface with best fit with Freundlich isotherm and pseudo-second-order model promoting combination of physical interaction (as confirmed from Dubinin–Radushkevich and Temkin model) dominated by solute-solid interactive forces (hydrogen boding, ion exchange and p–p stacking of aromatic ring with carbon nanotubes) responsible for EBT removal. The extracted thermodynamic parameters provide clear evidence that the adsorption of EBT onto nano-adsorbent is both exothermic and spontaneous. This categorization makes our prepared material an excellent choice for the removal of mutagenic dyes, especially at around room temperature under neutral pH conditions.

_Keywords:_ Eriochrome Black T; Multi-walled carbon nanotube; Montmorillonite; Point of zero charge; Isotherm; Thermodynamic

* Corresponding author.

# 1. Introduction

Nowadays, one of the most important environmental issue is related to water scarcity, water contamination and water quality. The problem of the treatment of contaminated wastewaters is of the upmost worldwide interest [1]. In many cases, water contamination is caused by discharging inorganic and/or organic compounds; particularly organic dyes in waters by effluents which must be avoided since they are toxic against life and normally accompanied by water coloration, resulting in low water quality besides secondary issue in the wastewater treatment [2,3]. It requires a concerted effort from government agencies, industries, and communities to implement effective solutions and ensure sustainable water management practices. To address this challenge, there is an urgent need to develop innovative waste treatment technologies and efficient methods that can mitigate these concerns and meet the demands of a sustainable environment. Researchers worldwide have shown significant interest in developing proficient technologies for the treatment and removal of highly toxic contaminants [4–7]. Universally colored stuff with complex aromatic alignments and synthetic source are branded as dyes. Dyes can be grouped into different categories like acidic and basic dyes. Acid dye are generally used for silk, wool, modified acrylics and nylon dyeing. These are also used in cosmetics, paper, food, ink-jet printing and leather dyeing. The major classes of acid dyes are azine, xanthene, anthraquinonoid, triphenylmethane, nitroso, nitro and azo dyes. Basic dyes are water soluble and comprise cyanine, thiazine, and acridine. Diazahemicyanine and triarylmethane and are famous for modified polyesters, nylons, poly acrylonitrile as well as paper industry and medicines. Many health impairments like teratogenesis, mutagenesis, and allergies as well as cancer are caused by contact with these dyes [8–11]. Thus, making it imperative to treat colored wastewaters from offender industries before discharging into the environment [12].

Several methods of dye removal from wastewater including biological, chemical, and physical methods have been used for the extraction of dyes from aqueous solutions [10]. Biological methods, though effective but time consuming, chemical methods on the other hand necessities the use of costly chemicals rendering them economically unrealizable for industrial-scale applications [13]. Various physical methods including adsorption, electrochemistry, membrane treatment and bioremediation, membrane filtration and reverse osmosis, are also commonly used [8], however adsorption is widely regarded as a competitive treatment technology for colored pollution in aqueous environments due to its wide applicability and ease of operation [6]. Nano-adsorbents are type of materials that, due to their properties and adsorption capacities, have applications in the removal of organic dyes from waters. Inclusive of these nanomaterials are carbon nanotubes (CNTs), grapheme sheets (GS), and metal oxides (MO). CNTs are made up of sp$^2$ hybridized carbons arranged as hollow cylindrical tubes with (1–100) nm diameter. These are commonly available in two forms, single-walled carbon nanotubes (SWCNTs) presented a diameter in the range of (0.4–10) nm and multi-walled carbon nanotubes (MWCNTs) spacing between sheets ranging from 0.34 nm to 0.38 [14–17]. The graphene sheets are rolled to form SWCNT, while multiple layers of concentric SWCNTs of different diameters held together by van der Waals forces form MWCNT [4]. Both SWCNT and MWCNT are emerging as potential sorbents due to their hollow cylindrical structure, high surface area, thermochemical robustness, high aspect ratio, mechanical strength and easy surface modification [6,7]. Particular attention has been devoted to the utilization of MWCNT as an adsorbent for the removal of dyes and heavy metals because of its cost-effectiveness [18]. Despite aforementioned advantages, the usage of CNTs remained limited due of their low solubility and adsorption capacities, aggregation of particles, difficult processing etc. [13]. Thus, to overcome these drawbacks and to enhance the adsorption efficacy, the pristine CNTs have been modified by either functionalization or fabrication of composites with various adsorbents such as metal oxide nanoparticles, chitosan, graphene, chitosan/bentonite composite and biomass. The need for treatment methods that are effective and economic is driving research interest towards adsorbents that are cheap, preferable naturally occurring like clays. It is witnessed from a wide range of consulted literature review that some clays have appreciable adsorption capacities besides being widely available. It is well established that structural and adsorption characteristics, that is, adsorption capacity, specific surface area, pore volume, grain size and pore size distribution of adsorbents play a crucial role in using them in various applications [8]. Montmorillonite clay (MC) is a natural substance that is frequently used as an adsorbent to eliminate diverse organics and inorganics toxins. MC has a number of chattels particularly non-toxicity, high surface area, low price, high sorption capability, eco-benign rendering it proficient adsorbent for dyes adsorption from aqueous media. Based upon extensive literature survey, to the best of our understanding no exertion is undertaken so far on the removal of Eriochrome Black T (EBT) onto functionalized MC based CNT nanocomposite from aqueous phase. EBT is a notorious azo dye extensively used in dye producing industries and its degradation leads to cancer-causing phenolic constituents which are hard to be exterminated by biological tools due to benzene building blocks [19]. Based upon extensive literature survey, to the best of our understanding no exertion is undertaken so far on the removal of EBT onto functionalized MC based CNT nanocomposite from aqueous phase. EBT is a notorious azo dye extensively used in dye producing industries and its degradation leads to cancer-causing phenolic constituents which are hard to be exterminated by biological tools due to benzene building blocks. Dye stuff removal from wastewater has been a matter of concern, both from aesthetic sense and health point of view. Color removal from textile effluents on industrial scale has been given much attention in the last few years, not only due to its possible toxicity, but also because of its visible problems. Adsorption can be employed as low-cost alternatives for recalcitrant dye removal from industrial wastewater, therefore the need for adsorbents that are cheap, preferable naturally occurring like clays is highly driving research interest. The use of clay-based materials over commercially available adsorbents is economical due to their low-cost, abundant availability, non-toxicity and potential for ion exchange. The main focus of this research work is to functionalize and evaluate multi-walled

carbon nanotube modified montmorillonite (CNT/MMT) as an environmental benign remedy for wastewater treatment and optimize its operational parameters for the removal of EBT.

## 2. Experimental

### 2.1. Materials

All the chemicals used in this project were of analytical grade and were used without further purification. EBT of high purity was purchased from Sigma-Aldrich (Germany). Montmorillonite clay was procured from Aldrich chemicals while MWCNT was obtained from Alfa Aesar, United Kingdom. All solutions were prepared with Millipore (MILLIPORE Elix by Merck) deionized water.

### 2.2. Montmorillonite/carbon nanotube based adsorbent preparation

In a typical experiment 10 g of montmorillonite dispersed with distilled water was mixed with 5.5 g of MWCNT with the help of magnetic stirrer at room temperature till suitable viscosity and homogeneity. Afterwards the mixture was filtered and dried in an oven at 120°C for 12 h. The prepared CNT/MMT mass was then allowed to cool at room temperature and calcined at 650°C for one h to obtain the desired adsorbent.

### 2.3. Characterization of CNT/MMT derived adsorbent

In order to fully understand the mechanism of adsorption the prepared adsorbent was characterized before and after adsorption by the Fourier-transform infrared spectroscopy (FTIR) and scanning electron microscopy (SEM) and energy-dispersive X-ray spectroscopy designed by PerkinElmer, Hillsboro, Oregon, USA, respectively. The BET (Brunauer–Emmett–Teller) surface area was monitored by $N_2$ adsorption–desorption via Micromeritics ASAP 2020 instrument (USA) at 77 K. Adsorption efficiency was computed by engaging UV-Visible spectrophotometer (Shimadzu-1900) manufactured by Japan.

### 2.4. Batch adsorption studies

Using 50 mL of EBT solution in a 100 mL conical flask on a shaker at a speed of 100 rpm, batch adsorption experiment was conducted to remove the dye. The initial dye concentration was set at 5–30 ppm, the adsorbent dosage was varied from 0.1 to 1 g, and the adsorption time ranged from 15 to 60 min. The adsorption operations were carried out between 10°C to 50°C. CNT/MMT composite and dye effluent were separated from one another by filtration following each adsorption experiment. % adsorptive removal $E$ (%) and maximum uptake capacity, that is, $q_e$ (mg/g) of EBT was estimated by using Eqs. (1) and (2) by engaging external calibration curve of EBT with different working solutions of EBT.

$$E\left(\%\right) = \frac{\left(C_i - C_f\right)}{C_i} \times 100 \tag{1}$$

$$q_e\left(\mathrm{mg/g}\right) = \frac{V\left(C_i - C_f\right)}{W} \tag{2}$$

where $C_i$ is the initial concentration (ppm) of EBT, $C_f$ is the final concentration, $V$ is the solution volume (L) while $V$ is the weight of adsorbent in gram.

## 3. Results and discussion

### 3.1. BET surface area analysis of CNT/MMT composite before and after adsorption

The surface area is a critical physical parameter that plays a decisive role in adsorption. It also provides essential insights into the interactions of molecules and ions that will be adsorbed onto the surface. BET surface area examination of the prepared nanocomposite recorded Type II adsorption isotherm with $S_{\mathrm{BET}}$ as 250 m²/g which increases to 265 m²/g after adsorption of dye. Such increase in specific surface area is in agreement with already documented literature on heavy metals adsorption by modified clay [20].

### 3.2. SEM analysis of CNT/MMT composite before and after adsorption

Fig. 1 shows the SEM image of prepared CNT/MMT adsorbent. From Fig. 1 it is clarified that composite adsorbent possess aggregated morphology with smaller particles having coarse flat type spongy surface reflecting perfect enhanced adsorption capacity of the engaged adsorbent. Figs. 2 and 3 expose the elemental composition and particle size distribution correspondingly. The particle size is roughly around 9 μm. Our findings on morphology is witnessed by other researchers [21]. The energy-dispersive X-ray spectroscopy (EDX) scan of CNT/MMT demonstrated the corresponding elements such as C, O, Mg, Al, Fe, K and Si. Fig. 4 suggests that after EBT adsorption particles stick together to give larger plates with decreased surface activity.

Fig. 5 represents the EDX spectrum of CNT/MMT nanocomposite after adsorption. The EDX image shows elemental composition of adsorbent after adsorption which
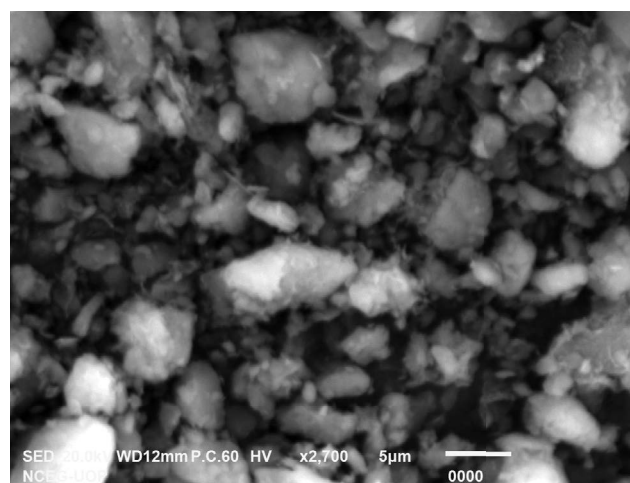


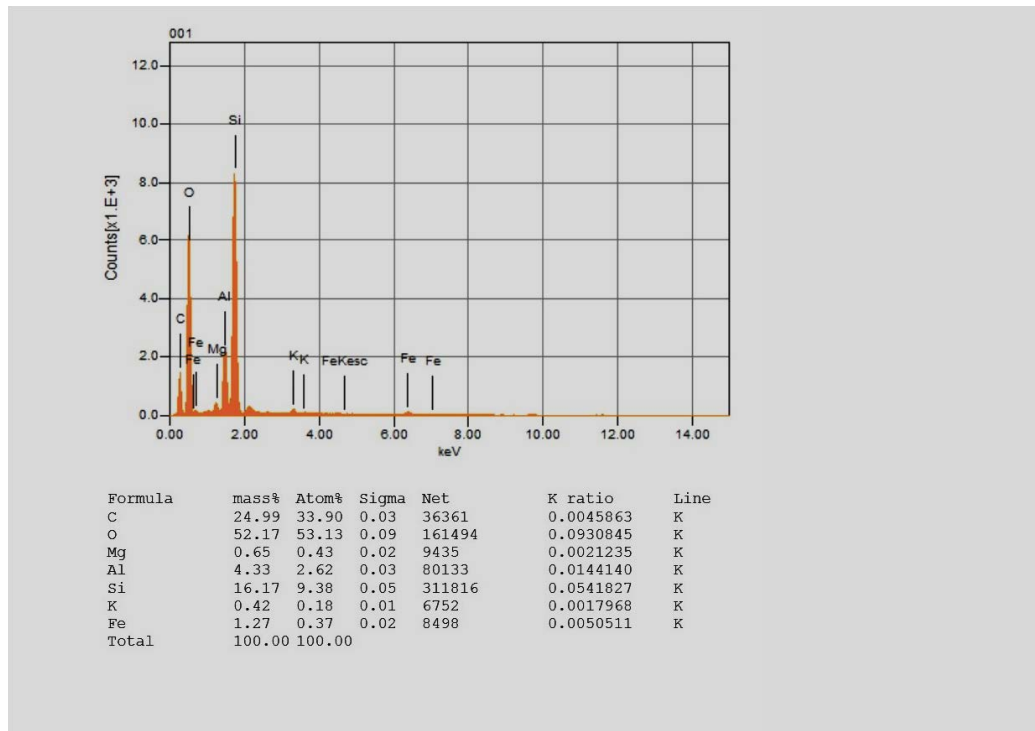Fig. 1. Scanning electron microscopy image of CNT/MMT composite before adsorption.

Fig. 2. Energy-dispersive X-ray spectroscopy image of CNT/MMT composite.
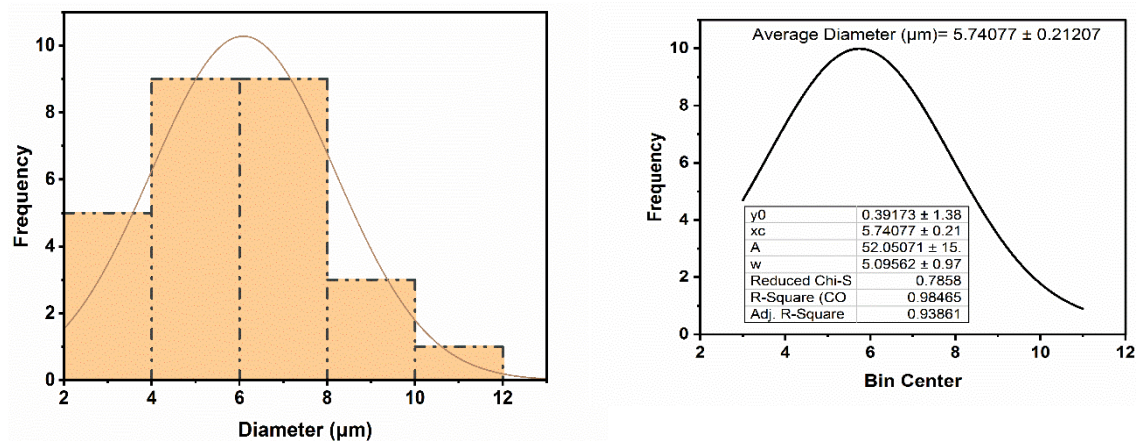


Fig. 3. Histogram of CNT/MMT composite particles distribution.

endorses an increase in carbon content from 24.99% by mass to 26.91% signifying adsorption of organic dye onto adsorbent surface. This also clarifies that adsorption is based on weak physical interaction.

### 3.3. FTIR analysis of CNT/MMT composite before and after adsorption

Studies on functional groups were ascertained via FTIR analysis which is presented as Fig. 6. Table 1 depicts peak positioning with assigned functional groups. From Fig. 6 it is witnessed that numerous functional groups namely unsaturated hydrocarbons, hydroxyl groups, alkyene, alkenes and silicon were exposed. Peak positiating at 3,456 cm$^{-1}$ can be attributed to –OH stretching vibrations prospecting that EBT interaction with –OH is responsible for the adsorptive removal of EBT. The band around 1,458 cm$^{-1}$ indicates the presence of vibrations that stretch the C and H atoms while bands positioned at 1,049; 601 and 570 cm$^{-1}$ refer to the presence of silicon compound. Comparing Fig. 6BA with 6AA reveals that peaks due to –OH, C–H and Si–O are affected upon adsoprtive removal of EBT while C=C functionalities are intensified thus highliting that adsoprtion mechanism pivots around –OH and Si–O interaction with EBT.

### 3.4. Thermogravimetric analysis/differential thermal analysis studies of CNT/MMT composite before adsorption

Fig. 7 illustrates the thermal stability curve of CNT/MMT composite. It is clear from Fig. 7 that initially 18% weight loss around 72°C is due to the removal of physiosorbed water beyond which our prepared nano-adsorbent is highly stable in the given temperature range. The corresponding derivative weight confirms this fact by single endothermic peak, reflecting elimination of physically adsorbed water/moisture content.
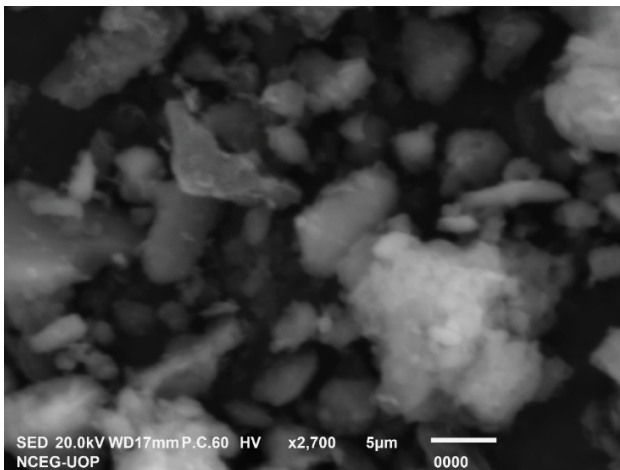


Fig. 4. Scanning electron microscopy image of CNT/MMT composite after adsorption.

### 3.5. Optimization of pH and point of zero charge studies

Point of zero charge (PZC) is the value of pH at which the components of surface charge are equal to zero for specified conditions. It does not mean that there is no charge at the surface for pH of PZC, but there are equal amounts of both negative and positive charges. For PZC studies, 50 mL of different pH solutions were prepared using 0.1 M (HCl and NaOH) and 0.2 g of adsorbent was added to each flask and shaken for 30 min and equilibrated for 24 h. Final pH was determined and ΔpH was calculated by the difference of final and initial pH. Fig. 8 shows typical PZC curve which exhibits 4.2 as the required PZC while Fig. 9 displays variation of $q_e$ (mg/g) against varying pH. An examination of the curve reveals that pH 4.5 and 7 give almost parallel adsorption efficacy so further experiments were conducted at pH 7 which is mimicking somehow natural conditions.

### 3.5. Studies on initial EBT concentration optimization

In order to study the relationship between the initial dye concentration and adsorption capacities, different working solutions 5, 10, 15, 25 and 30 ppm was prepared and their absorbance was determined by UV-Vis spectrophotometer (Shimadzu-1900, Japan) to plot calibration curve as shown as Fig. 10.

In order to study the influence of EBT initial concentration on adsorption, batch adsorption studies were conducted with 50 mL of different initial concentration 5, 10, 15, 25 and 30 ppm of EBT having 0.5 g of CNT/MMT for 30 min shaking duration. Remaining concentration after adsorption was estimated using slope of calibration curve.



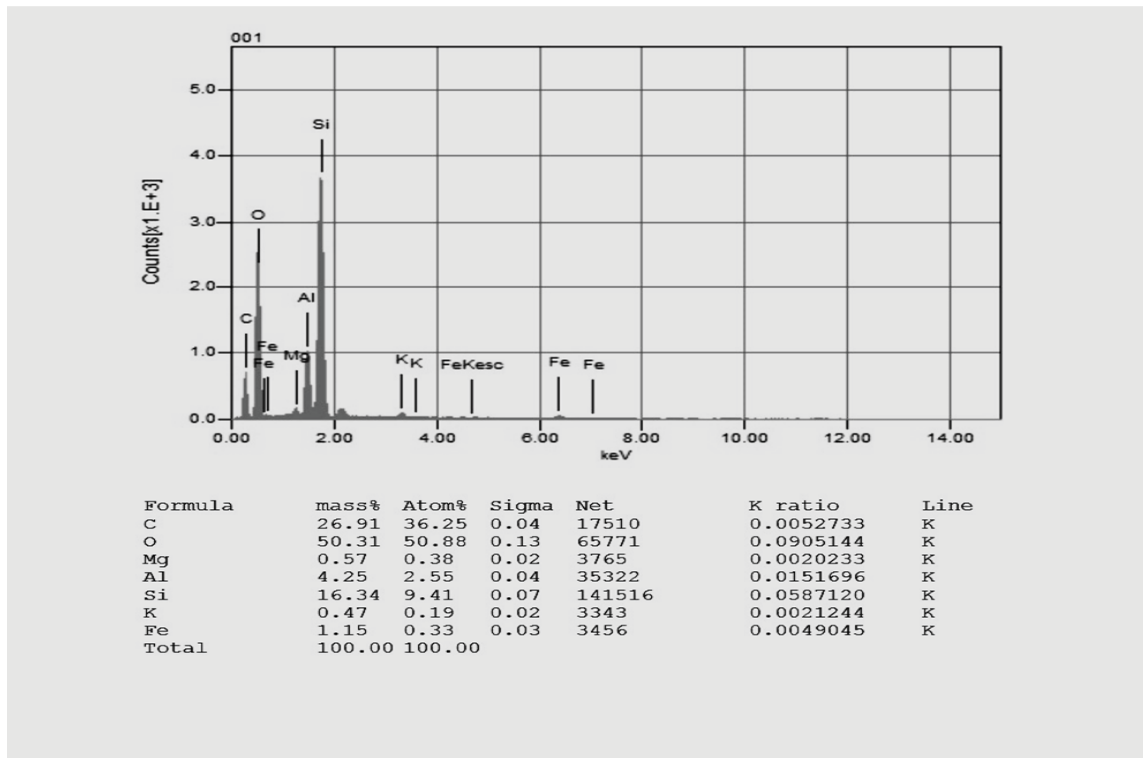| Formula | mass% | Atom% | Sigma | Net | K ratio | Line |
|---------|-------|-------|-------|------|---------|------|
| C | 26.91 | 36.25 | 0.04 | 17510 | 0.0052733 | K |
| O | 50.31 | 50.88 | 0.13 | 65771 | 0.0905144 | K |
| Mg | 0.57 | 0.38 | 0.02 | 3765 | 0.0020233 | K |
| Al | 4.25 | 2.55 | 0.04 | 35322 | 0.0151696 | K |
| Si | 16.34 | 9.41 | 0.07 | 141516 | 0.0587120 | K |
| K | 0.47 | 0.19 | 0.02 | 3343 | 0.0021244 | K |
| Fe | 1.15 | 0.33 | 0.03 | 3456 | 0.0049045 | K |
| Total | 100.00 | 100.00 | | | | |

Fig. 5. Energy-dispersive X-ray spectroscopy image of CNT/MMT composite after Eriochrome Black T adsorption.
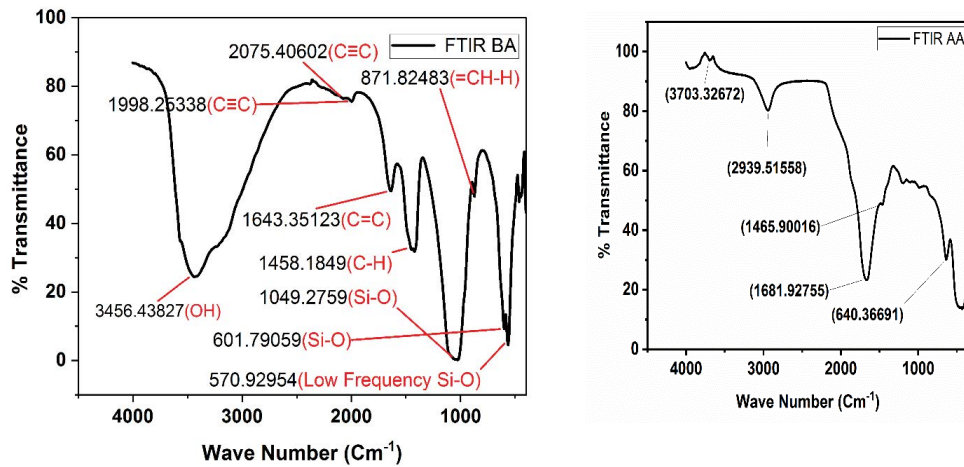
Fig. 6. Fourier-transform infrared spectrum of CNT/MMT composite before adsorption (BA) (a) and after adsorption (AA) (b).

Table 1
Peaks positions with assigned functional groups in Fourier-transform infrared spectroscopy scan of CNT/MMT composite

| Peak position (cm$^{-1}$) | Functional group assigned |
| --- | --- |
| 3,456.43827 | O–H stretching vibration |
| 2,075.40602 | C≡C alkynes |
| 1,998.25338 | C≡C alkynes |
| 1,643.35123 | C=C alkenes |
| 1,458.1849 | C–H bending |
| 1,049.2759 | Si–O silicon compound |
| 871.82483 | =CH–H |
| 601.79059 | Si–O silicon compound |
| 570.92954 | Si–O (low frequency silicon compound) |
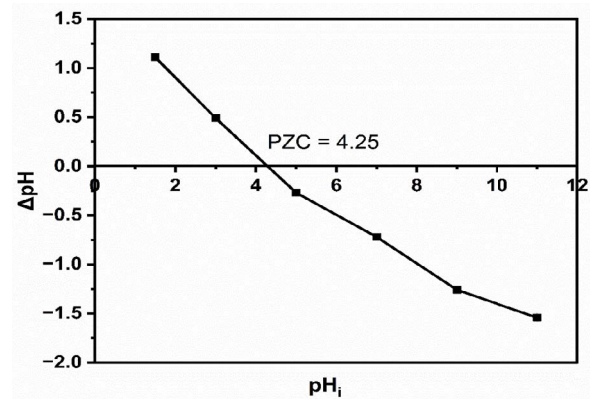


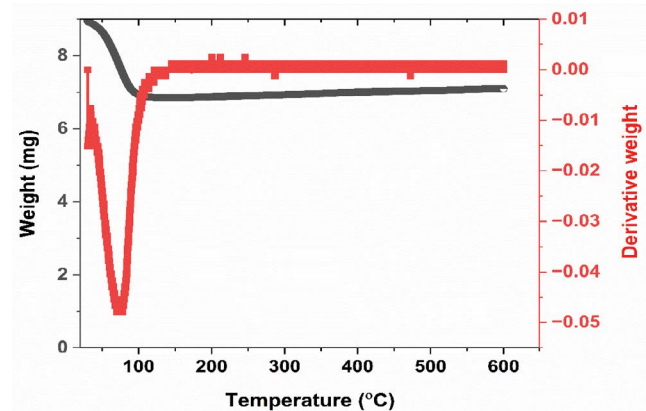Fig. 8. Plot showing point of zero charge of CNT/MMT composite.



Fig. 7. Thermogravimetric analysis/differential thermal analysis scan of CNT/MMT composite.
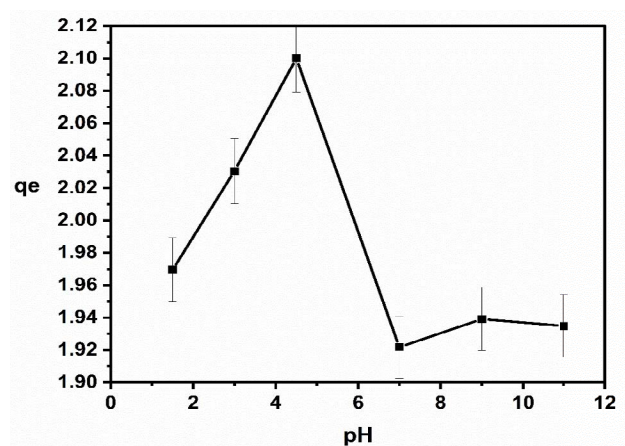


Fig. 9. Uptake removal capacity of Eriochrome Black T against varying pH.

Pictorial description of initial dye concentration on percent removal and adsorption capacity is represented as Figs. 11 and 12 exclusively. It is clear from Figs. 11 and 12 that initially adsorptive removal capacity increases with increasing EBT initial concentration due to pressure inclined generated motivating force till it boosted at 25 ppm with 1.6 mg/g

uptake ability confirming saturation level at 25 ppm of EBT. So, this concertation was selected as model for further investigation. This trend of initially increase in dye elimination is in close agreement with previous findings [22,23].
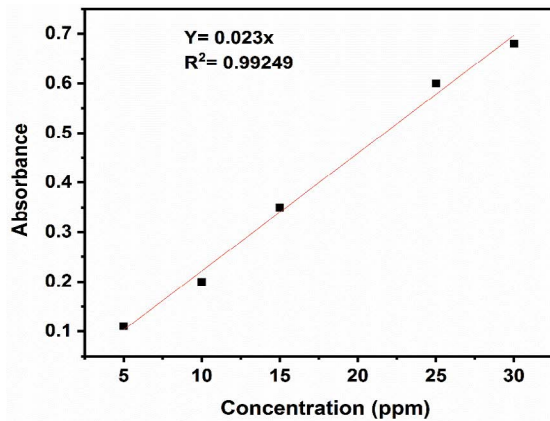
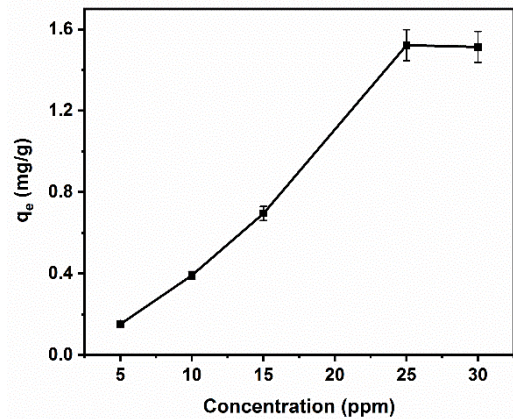Fig. 10. Calibration curve of Eriochrome Black T.



Fig. 12. Removal uptake capacity of Eriochrome Black T against varying initial concentration.
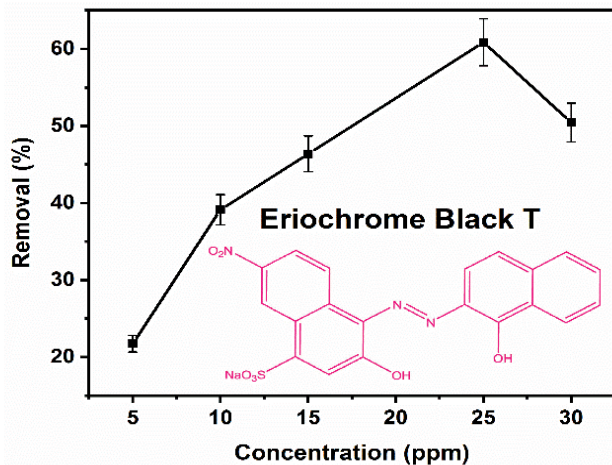


Fig. 11. % removal of Eriochrome Black T against various initial concentration.
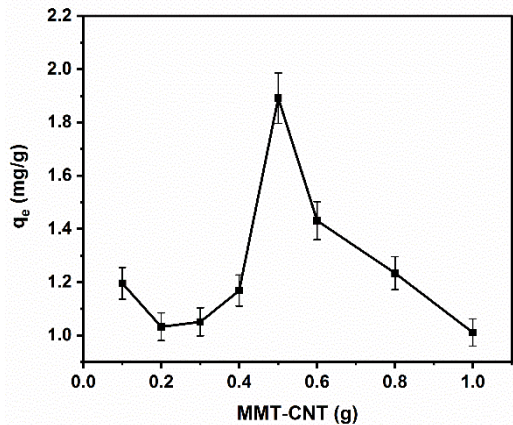


Fig. 13. Removal uptake capacity of Eriochrome Black T against varying CNT/MMT dosage.

### 3.6. Optimization of CNT/MMT dosage

An essential factor in estimating the adsorbent capacity for a specific amount of adsorbent under operating conditions is the amount of adsorbent. The notion for the adsorption process, which is economically viable, is shown by the effect of the amount of adsorbent material. Absorbance after adsorption when different doses 0.1–1.0 g of CNT/MMT were added to 50 mL of 25 ppm EBT solutions and shaken for 30 min were determined and then. $q_e$ value for each solution was calculated from absorbance using slope of the calibration curve. Fig. 13 clarifies that $q_e$ value progresses linearly till it levelled off at 0.5 g giving 1.891304 mg/g (82%) adsorptive removal tendency. This could be attributed to the saturation of surface area, volume and active sites availability. Hence 0.5 g CNT/MMT was marked as perfect choice for consequent studies. The same behavior is reported by earlier researchers in the same area [24].

### 3.7. Optimization of temperature

In order to investigate the effect of temperature onto the adsorptive removal of EBT dye at neutral pH, 30 min shaking time with 0.5 g of CNT/MMT and 25 ppm of EBT, batch

adsorption experiments were conducted at a range of temperatures 30°C–50°C. Fig. 14 exhibits recorded observations. Fig. 14 exposes that adsorptive removal capacity is perceived towards negative direction with increasing temperature hence confirming 2.05 mg/g uptake capacity with 82% EBT elimination at model temperature, that is, 30°C. Our recorded uptake capacity is higher than earlier studies with same dye on activated carbon derived from cannabis under similar pH condition [25]. This observation demonstrates exothermicity of the targeted process hence suggesting CNT/MMT as an efficient cost-effective choice around room temperature operations. This decreasing trend in adsorption capacity with increasing temperature is also observed by other researchers [26].

### 3.8. Optimization of shaking time

The adsorption process is substantially influenced by the contact time. Contact time can also effect the adsorption kinetics beside economic efficiency. Contact time is therefore another performance-determining factor in the adsorption process. Fig. 15 displays % removal and $q_e$ (mg/g) derived from the slope of the curve drawn from absorbance after adsorption at various shaking times (15–60 min) with 0.5 g

of CNT/MMT in 50 mL of 25 ppm EBT solutions at neutral pH and adjusted temperature of 30°C. Fig. 15 unveils that the amount of dye that the CNT/MMT composite was able to extract from an aqueous solution upsurges as the adsorption period prolonged to 30 min. Beyond this time, less EBT dye was removed, verifying that 30 min is the appropriate length of time for the adsorption equilibrium. The presence of active sites on the surface of the CNT/MMT composite is contributed to the initial and rapid rise in dye removal within the first 30 min. After 30 min of adsorption, vacant active sites were filled up by adsorbate molecules. Tables 2a and b show the worth of our utilized nano-adsorbent in comparison with formerly engaged adsorbent.

### 3.9. Kinetics studies of EBT removal onto CNT/MMT composite

In order to fully understand the mass transfer and rate controlling phases in real time application of CNT/MMT

as an adsorbent, it is imperative to undertake adsorption kinetic studies. Adsorption data under investigated ideal parameters were fitted to two well established kinetic models namely pseudo-first-order and pseudo-second-order kinetic model as per given Eqs. (3) and (4), individually.

$$\ln\left(q_e - q_t\right) = \ln q_e - k_1 t \tag{3}$$

$$\frac{t}{q_t} = \frac{1}{k_2 q_e^2} + \frac{t}{q_e} \tag{4}$$

where $q_e$ and $q_t$ refers to the adsorption capacity (mg/g) at equilibrium and at any time $t$ separately, while $k_1$ and $k_2$ denotes rate constant for first and second-order kinetic reaction as per written order. Figs. 16 and 17 present visual representations of the kinetic analysis of adsorption using the
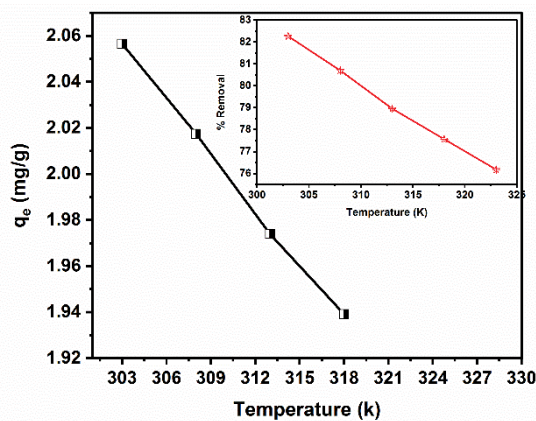


Fig. 14. Removal uptake capacity of Eriochrome Black T against varying temperatures, inset showing % removal vs. temperature.
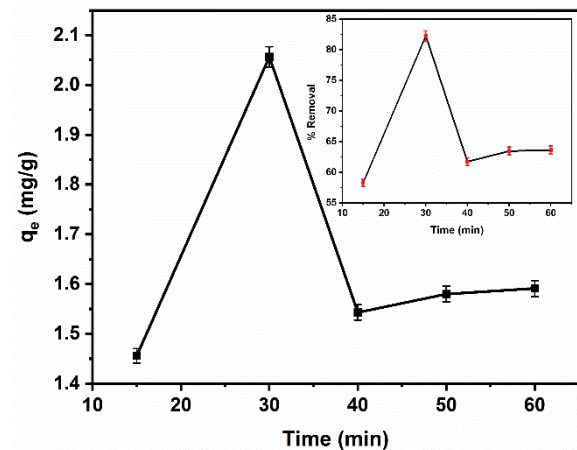


Fig. 15. Removal uptake capacity of Eriochrome Black T against varying time, inset showing % removal vs. time.

Table 2a
Comparative % removal of Eriochrome Black T dye at equilibrium contact time onto different adsorbents

| Adsorbent | Equilibrium time (min) | Removal (%) | References |
|---|---|---|---|
| Acid modified graphene | 180 | 80 | [27] |
| Waste hemp activated carbon | 180 | 62 | [25] |
| Expanded perlite | 80 | 91.5 | [28] |
| Doum fruit as a natural adsorbent | 30 | 83.3 | [29] |
| CNT/MMT | 30 | 82 | Present study |

Table 2b
Comparative (uptake capacity) $q_e$ (mg/g) of Eriochrome Black T dye at equilibrium contact time onto different adsorbents

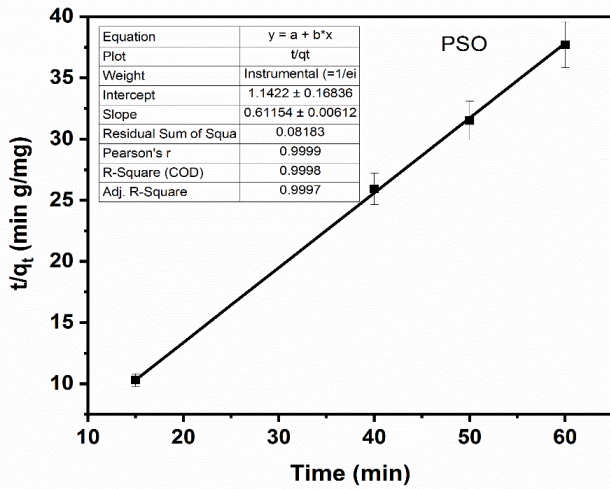| Adsorbent | $q_e$ (mg/g) | References |
|---|---|---|
| Rice hull-based activated carbon | 2.0 | [30] |
| Bentonite carbon composite | 0.091 | [31] |
| Alginate/basil seed mucilage biocomposite | 2.80 for 10 mg/L and 1.09 for 15 mg/L initial dye concentration | [32] |
| Yam peel activated carbon | 3.8 | [33] |
| CNT/MMT | 2.1 | Present study |

Fig. 16. Pseudo-second-order kinetic model of Eriochrome Black T adsorption.
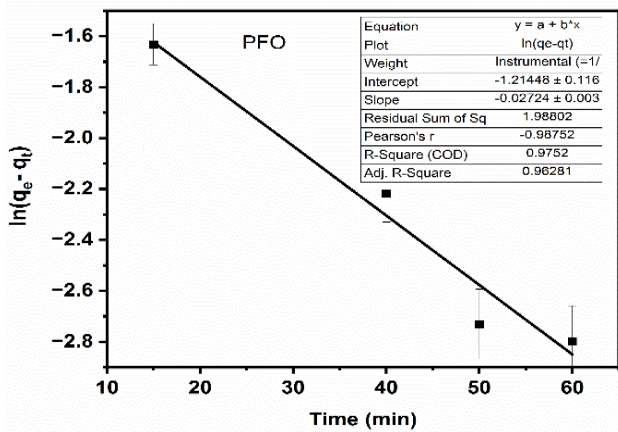


Fig. 17. Pseudo-first-order kinetic model of Eriochrome Black T adsorption.

provided equations. These figures validate that the pseudo-second-order model exhibits a higher $R^2$ value of 0.9998, along with the same uptake capacity as the theoretical value, specifically 1.64 mg/g for $q_e$(cal) and $q_e$(theo). In contrast, the pseudo-first-order model shows $R^2$ value of 0.962 with negative slope and intercept. These findings indicate that the pseudo-second-order model provides a superior description of EBT adsorption onto the CNT/MMT composite. The prevalence of weak interactive forces owing to solute-solid interactive forces (hydrogen boding, ion exchange and p–p stacking of aromatic ring with CNT) responsible for EBT removal is suggested by the pseudo-second-order model, with a rate constant $k_2$ of 0.33 g/mg·min, which was extracted from the intercept. Our findings on pseudo-second-order kinetics are endorsed by previous researchers with EBT on activated carbon from waste hemp [25] (Table 3).

### 3.10. Adsorption isotherms studies

To determine the suitability of CNT/MMT for the sorption capacity of EBT, the experimental data was modelled

Table 3
Kinetic parameters for adsorption of Eriochrome Black T onto CNT/MMT

| | |
|---|---|
| $q_e$(cal) (mg/g) | 1.64 |
| $k_2$ (g/mg·min) | 0.33 |
| $R^2$ | 0.9998 |

by fitting it to the Freundlich and Langmuir isothermal models, as represented by Eqs. (5) and (6), respectively.

$$\ln q_e = \ln k_f + \frac{1}{n}\ln C_e \tag{5}$$

$$\frac{C_e}{q_e} = \frac{1}{q_m K} + \frac{C_e}{q_m} \tag{6}$$

where $1/n$ and $k_f$ (mg/g/ppm)$^{1/n}$ expresses sorption ability and the energy for Freundlich model and $q_m$ is the adsorption capacity for monolayer coverage and $K$ (L/mg) is the Langmuir constant linked with adsorption equilibrium. Adsorption isothermal parameters were obtained at initial dye concentrations in the range of 5–30 ppm. The findings of the adsorption experiments demonstrated that the CNT/MMT composite is bestowed with greater EBT removal efficacy of 82%. The collected adsorption data was found to be best suited by the Freundlich isotherm (Fig. 18) as supported by higher $R^2$ value for the Freundlich isotherm as 0.9909 unlike 0.7288 for Langmuir model (19) with a negative slope. The behavior of the best fit using the Freundlich model indicates that CNT/MMT exhibits a heterogeneous surface state, implying the likelihood of EBT physisorption onto the CNT/MMT material. The value of $n$ (0.6) as obtained by the reciprocal of slope of Freundlich isotherm, is less than one showing high adsorption at low EBT concentration probably due to solute/solute interaction on the surface due to cooperative adsorption of EBT [34,35].

### 3.11. Dubinin–Radushkevich model

To demarcate adsorption process as chemisorption or physical adsorption, Dubinin–Radushkevich isotherm model was employed as this model does not assume a homogenous surface or constant sorption potential as other models. The linear form of Dubinin–Radushkevich isotherm can be written by Eqs. (7)–(9):

$$\ln q_e = \ln q_m - \beta\varepsilon^2 \tag{7}$$

$$\varepsilon = RT\ln\left(1 + \frac{1}{C_e}\right) \tag{8}$$

$$E = \frac{1}{\sqrt{2\beta}} \tag{9}$$

where $q_e$ is the equilibrium adsorption capacity (mg/g) while $q_m$ is the theoretical saturation capacity (mol/g), $\beta$ is adsorption energy related constant (kJ/mol) while $\varepsilon^2$ is the Polanyi potential. Fig. 20 exhibits a plot of $\ln q_e$ against
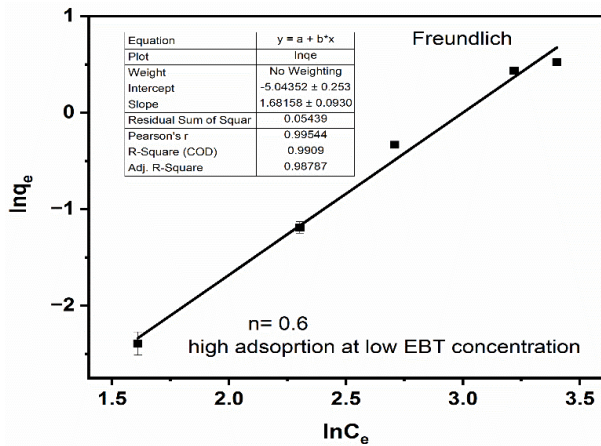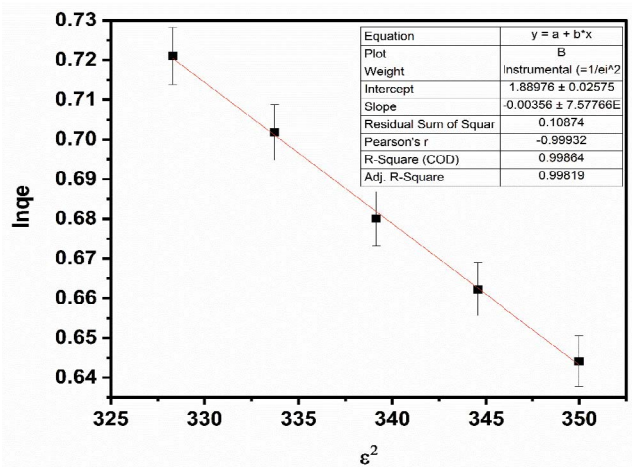
Fig. 18. Freundlich adsorption isotherm.



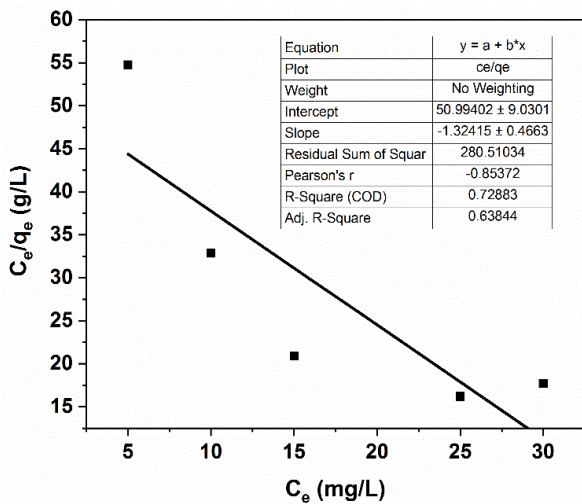Fig. 20. Dubinin–Radushkevich adsorption isotherm.



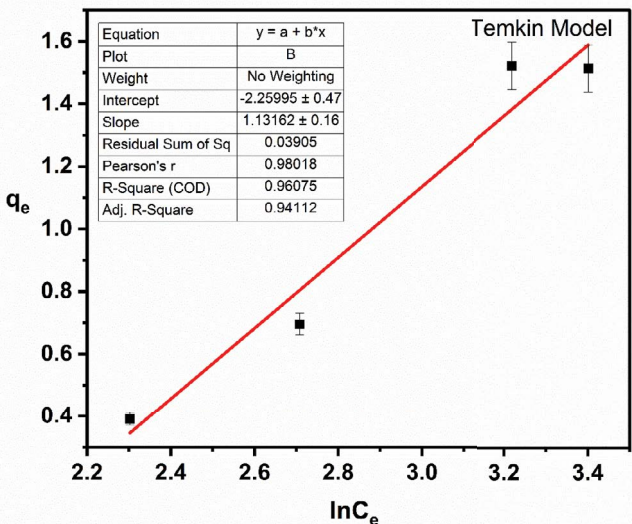Fig. 19. Langmuir adsorption isotherm.



Fig. 21. Temkin adsorption isotherm.

$\varepsilon^2$ resulting in a straight line with slope equal to $B$ (0.0036) and intercept giving value of 1.892. From the value of intercept, $q_m$ is estimated having value of 6.63 mol/g. As per Eq. (9), the average free energy of adsorption was estimated as 11.57 kJ/mol which is suggestive of predominance of physical adsorption as already supported by best fit with Freundlich adsorption isotherm. Our findings are fully buttressed by previous work of similar nature [36,37].

### 3.12. Temkin adsorption isotherm

The Temkin isotherm model is based upon assumption that heat of adsorption decreases linearly rather than logarithmically with the increase in coverage of the adsorbent surface, and that adsorption is characterized by a uniform distribution of binding energies, up to a maximum binding energy. The Temkin isotherm can be well described by Eq. (10):

$$q_e = \frac{RT}{b} \ln K_T + \frac{RT}{b} \ln C_e \tag{10}$$

where plot of $q_e$ vs. $\ln C_e$ gives straight line with a slope equal to $RT/b$ from which Temkin constant ($b$) can be computed as 2,189.441 J/mol, similarly the equilibrium binding constant $K_T$ was estimated as 0.1357 L/g from intercept of the plot as shown in Fig. 21. The achieved 0.1357 as equilibrium binding constant exposes adsorption as physical interaction in nature.

### 3.13. Thermodynamic studies

The thermodynamic investigation of dye adsorption with CNT/MMT involved the evaluation of key thermodynamic parameters, namely adsorption equilibrium constant, change in Gibbs free energy ($\Delta G°$), change in enthalpy ($\Delta H°$), and change in entropy ($\Delta S°$). These parameters were calculated using Eqs. (11)–(13):

$$K_d = \frac{q_e}{C_e} \tag{11a}$$

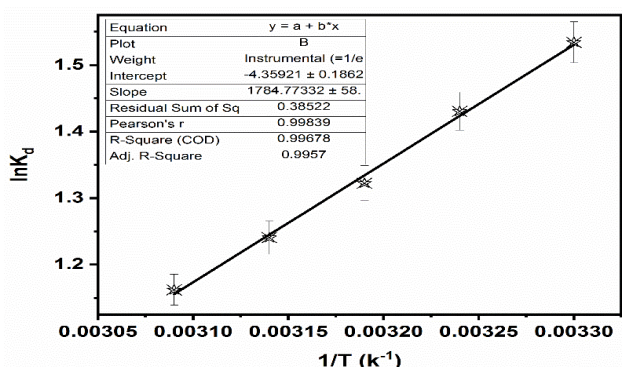| Equation | y = a + b*x |
|---|---|
| Plot | B |
| Weight | Instrumental (=1/e |
| Intercept | -4.35921 ± 0.1862 |
| Slope | 1784.77332 ± 58. |
| Residual Sum of Sq | 0.38522 |
| Pearson's r | 0.99839 |
| R-Square (COD) | 0.99678 |
| Adj. R-Square | 0.9957 |

Fig. 22. $1/T$ against $\ln K_d$ curve for Eriochrome Black T adsorption.

Table 4
Thermodynamic parameters for adsorption of Eriochrome Black T onto CNT/MMT

| $\Delta G$ (kJ/mol) | | | | | $\Delta H$ (kJ/mol) | $\Delta S$ (J/mol·K) |
|---|---|---|---|---|---|---|
| 303 K | 308 K | 313 K | 318 K | 323 K | −14.83 | −36.24 |
| −3.86 | −3.66 | −3.44 | −3.27 | −3.12 | | |

$$K_d = \frac{\Delta S^\circ}{R} - \frac{\Delta H^\circ}{RT} \tag{11b}$$

$$\Delta G^\circ = -RT \ln K_d \tag{12}$$

$$\Delta G^\circ = \Delta H^\circ - T\Delta S^\circ \tag{13}$$

where $K_d$ is the equilibrium adsorption constant, $q_e$ is the amount of dye adsorbed on the surface of adsorbent and $C_e$ is the equilibrium concentration of dye after adsorption. By analyzing the plot of $1/T$ vs. $\ln K_d$ as shown in Fig. 22, the values of the change in enthalpy ($\Delta H$) and change in entropy ($\Delta S$) were individually extracted from the slope and intercept, respectively. The thermodynamic parameters obtained and presented in Table 4 provide clear evidence that the adsorption of EBT onto CNT/MMT is both exothermic and spontaneous as the values of $\Delta G$ and $\Delta H$ are below −20 kJ/mol [38]. The negative $\Delta H$ is depictive of interaction between the adsorbent surface and EBT as already endorsed by the best fit with pseudo-second-order kinetic model. Positive $\Delta S$ value illustrates that increasing temperature boosts the adsorption effectiveness at adsorbent/adsorbate interface probably due to fortuitous occurrences at interface. This categorization makes our prepared material an excellent choice for the removal of mutagenic dyes, especially at around room temperature and neutral pH conditions.

## 4. Conclusion

In this study, we addressed the urgent environmental concern of non-biodegradable organic dyes by examining the adsorption behavior of EBT with CNT/MMT composite. Batch adsorption studies revealed a maximum EBT removal of 82% at 30°C, with favorable adsorption onto the composite's heterogeneous surface, driven by combination of weak interactive forces. The material proved to be an excellent choice for removing mutagenic dyes under neutral pH and room temperature conditions, making it a promising eco-friendly solution for dye-contaminated wastewater remediation.

## Acknowledgment

## References

[1] M. Afsharnia, H. Biglari, A. Javid, F. Zabihi, Removal of Reactive Black 5 dye from aqueous solutions by adsorption onto activated carbon of grape seed, Iran. J. Health Sci., 5 (2017) 48–61.

[2] N. Jahan, M. Tahmid, A.Z. Shoronika, A. Fariha, H. Roy, Md. N. Pervez, Y. Cai, V. Naddeo, Md. S. Islam, A comprehensive review on the sustainable treatment of textile wastewater: zero liquid discharge and resource recovery perspectives, Sustainability, 14 (2022) 15398, doi: 10.3390/su142215398.

[3] J. Wang, L. Chu, L. Wojnárovits, E. Takács, Occurrence and fate of antibiotics, antibiotic resistant genes (ARGs) and antibiotic resistant bacteria (ARB) in municipal wastewater treatment plant: an overview, Sci. Total Environ., 744 (2020) 140997, doi: doi: 10.1016/j.scitotenv.2020.140997.

[4] Y. Zhou, Y. Fang, R.P. Ramasamy, Non-covalent functionalization of carbon nanotubes for electrochemical biosensor development, Sensors (Basel), 19 (2019) 392, doi: 10.3390/s19020392.

[5] H. Eyni, H. Tahermansouri, F. Kiani, M. Jahangiri, Kinetics, equilibrium and isotherms of Pb²⁺ adsorption from aqueous solutions on carbon nanotubes functionalized with 3-amino-5a,10a-dihydroxybenzo[b] indeno [2,l-d]furan-10-one, New Carbon Mater., 34 (2019) 512–523.

[6] N. Bagotia, V. Choudhary, D.K. Sharma, Synergistic effect of graphene/multi-walled carbon nanotube hybrid fillers on mechanical, electrical and EMI shielding properties of polycarbonate/ethylene methyl acrylate nanocomposites, Composites, Part B, 159 (2019) 378–388.

[7] D.K. Sharma, N. Bagotia, Production of graphene and carbon nanotubes using low-cost carbon-based raw materials and their utilization in the production of polycarbonate/ethylene methyl acrylate-based nanocomposites, Indian J. Eng. Mater. Sci., 27 (2021) 1127–1135.

[8] M. Kaykhaii, M. Sasani, S. Marghzari, Removal of dyes from the environment by adsorption process, Chem. Mater. Eng., 6 (2018) 31–35.

[9] A. Kausar, M. Iqbal, A. Javed, K. Aftab, H.N. Bhatti, S. Nouren, Dyes adsorption using clay and modified clay: a review, J. Mol. Liq., 256 (2018) 395–407.

[10] T. Ngulube, J.R. Gumbo, V. Masindi, A. Maity, An update on synthetic dyes adsorption onto clay-based minerals: a state-of-art review, J. Environ. Manage., 191 (2017) 35–57.

[11] M.R. Samarghandi, M. Zarrabi, A. Amrane, M.N. Sepehr, M. Noroozi, S. Namdari, A. Zarei, Kinetic of degradation of two azo dyes from aqueous solutions by zero iron powder: determination of the optimal conditions, Desal. Water Treat., 40 (2012) 137–143.

[12] A. Kanwal, H.N. Bhatti, M. Iqbal, S. Noreen, Basic dye adsorption onto clay/MnFe₂O₄ composite: a mechanistic study, Water Environ. Res., 89 (2017) 301–311.

[13] M.T. Amin, A.A. Alazba, M. Shafiq, LDH of NiZnFe and its composites with carbon nanotubes and data-palm biochar with efficient adsorption capacity for RB5 dye from aqueous solutions: isotherm, kinetic, and thermodynamics studies, Curr. Appl. Phys., 40 (2020) 90–100.

[14] Y. He, X. Fu, H. Wu, T. Zhu, S. Li, B. Na, C. Peng, Highly efficient removal of methyl blue from aqueous solution using a novel

nitrogen-doped porous magnetic carbon, Desal. Water Treat., 173 (2020) 409–419.

[15] M. Azadfar, H. Tahermansouri, M. Qomi, The picric acid removal from aqueous solutions by multi-walled carbon nanotubes/EDTA/carboxymethylcellulose nanocomposite: central composite design optimization, kinetic, and isotherm studies, J. Chin. Chem. Soc., 68 (2021) 2103–2117.

[16] H. Tahermansouri, M. Beheshti, Kinetic and equilibrium study of lead(II) removal by functionalized multi-walled carbon nanotubes with isatin derivative from aqueous solutions, Bull. Korean Chem. Soc., 34 (2013) 3391–3398.

[17] N.N. Nia, M. Rahmani, M. Kaykhaii, M. Sasani, Evaluation of Eucalyptus leaves as an adsorbent for decolorization of Methyl Violet (2B) dye in contaminated waters: thermodynamic and kinetics model, Model. Earth Syst. Environ., 3 (2017) 825–829.

[18] A. Mittalb, M. Naushad, G. Sharma, Z.A. ALothman, S.M. Wabaidur, M. Alam, Fabrication of MWCNTs/ThO$_2$ nanocomposite and its adsorption behavior for the removal of Pb(II) metal from aqueous medium, Desal. Water Treat., 57 (2016) 21863–21869.

[19] G. Zeydouni, M. Kianizadeh, Y. Omidi Khaniabadi, H. Nourmoradi, S. Esmaeili, M.J. Mohammadi, R. Rashidi, Eriochrme Black-T removal from aqueous environment by surfactant modified clay: equilibrium, kinetic, isotherm, and thermodynamic studies, Toxin Rev., 38 (2019) 307–317.

[20] H. Lu, Q. Zhang, Y. Li. Dong, X. Zhang, The adsorption capacity, pore structure, and thermal behavior of the modified clay containing SSA, Adv. Mater. Sci. Eng., 2016 (2016) 9894657, doi: 10.1155/2016/9894657.

[21] S. Arellano-Cárdenas, S. López-Cortez, M. Cornejo-Mazón, J.C. Mares-Gutiérrez, Study of malachite green adsorption by organically modified clay using a batch method, Appl. Surf. Sci., 280 (2013) 74–78.

[22] V.K. Gupta, Application of low-cost adsorbents for dye removal–a review, J. Environ. Manage., 90 (2009) 2313–2342.

[23] O.O. Ololade, I.A. Ololade, O.O. Ajayi, N.A. Oladoja, F. Alomaja, F.F. Oloye, D.D. Akerele, Interactive influence of Fe–Mn and organic matter on pentachlorophenol sorption under oxic and anoxic conditions, J. Environ. Chem. Eng., 4 (2016) 1899–1909.

[24] S. Mustapha, D.T. Shuaib, M.M. Ndamitso, M.B. Etsuyankpa, A. Sumaila, U.M. Mohammed, M.B. Nasirudeen, Adsorption isotherm, kinetic and thermodynamic studies for the removal of Pb(II), Cd(II), Zn(II) and Cu(II) ions from aqueous solutions using *Albizia lebbeck* pods, Appl. Water Sci., 9 (2019) 1–11.

[25] F. El Mansouri, G. Pelaz, A. Morán, J.C.E. da Silva, F. Cacciola, H. El Farissi, J. Brigui, Efficient removal of Eriochrome Black T dye using activated carbon of waste hemp (*Cannabis sativa* L.) grown in Northern Morocco enhanced by new mathematical models, Separations, 9 (2022) 283, doi: 10.3390/separations9100283.

[26] L. Nahali, Y. Miyah, F. Mejbar, M. Benjelloun, O. Assila, Y. Fahoul, F. Zerrouq, Assessment of Brilliant Green and Eriochrome Black T dyes adsorption onto fava bean peels: kinetics, isotherms and regeneration study, Desal. Water Treat., 245 (2022) 255–269.

[27] A. Khalid, M. Zubair, A. Ihsanullah, Comparative study on the adsorption of Eriochrome Black T dye from aqueous solution on graphene and acid-modified graphene, Arabian J. Sci. Eng., 43 (2018) 2167–2179.

[28] J.M.F. Almeida, E.S. Oliveira, I.D.N. Silva, S.P.M.C. De Souza, N.S. Fernandes, Adsorption of Erichrome Black T from aqueous solution onto expanded perlite modified with orthophenanthroline, Rev. Virtual Quim., 9 (2017) 502–513.

[29] A.A. Abdel-Khalek, A. El-Hafiez, R.A. Mohamed, E. Gabrail, Insights into removal of Eriochrome Black T dye from aqueous solution by Doum fruit as a natural adsorbent, Egypt. J. Chem., 65 (2022) 189–199.

[30] M.D.G. de Luna, E.D. Flores, D.A.D. Genuino, C.M. Futalan, M.W. Wan, Adsorption of Eriochrome Black T (EBT) dye using activated carbon prepared from waste rice hulls—optimization, isotherm and kinetic studies, J. Taiwan Inst. Chem. Eng., 44 (2013) 646–653.

[31] F.M.S.E. El-Dars, H.M. Ibrahim, H.A. Farag, M.Z. Abdelwahhab, M.E.H. Shalabi, Adsorption kinetics of bromophenol blue and Eriochrome Black T using bentonite carbon composite material, Int. J. Sci. Eng. Res., 6 (2015) 1–14.

[32] V. Javanbakht, R. Shafiei, Preparation, performance of alginate/basil seed mucilage biocomposite for removal of Eriochrome Black T dye from aqueous solution, Int. J. Biol. Macromol., 152 (2020) 990–1001.

[33] M. Ladan, F.A. Usman, M.I. Maikudi, Removal of Erichrome Black T from aqueous solution using yam peel activated carbon, Bayero J. Pure Appl. Sci., 14 (2021) 198–205.

[34] O. Afzal, H.A. Alshammari, M.A. Altamimi, A. Hussain, B. Almohaywi, A.S. Altamimi, Hansen solubility parameters and green nanocarrier based removal of trimethoprim from contaminated aqueous solution, J. Mol. Liq., 361 (2022) 119657, doi: 10.1016/j.molliq.2022.119657.

[35] I. Kazeminezhad, A. Sadollahkhani, Photocatalytic degradation of Eriochrome Black T dye using ZnO nanoparticles, Mater. Lett., 120 (2014) 267–270.

[36] A.A. Inyinbor, F.A. Adekola, G.A. Olatunji, Kinetics, isotherms and thermodynamic modeling of liquid phase adsorption of Rhodamine B dye onto *Raphia hookerie* fruit epicarp, Water Resour. Ind., 15 (2016) 14–27.

[37] M. Azadfar, H. Tahermansouri, M. Qomi, Application of the graphene oxide/chitosan nanocomposite in the removal of methyl orange from aqueous solutions: a mechanism study, Indian J. Chem., 60A (2021) 209–219.

[38] A.M. Ayuba, M. Sani, Removal of Eriochrome Black T dye from aqueous solution using base activated typha grass (*Typha latifolia*) as an adsorbent, Bayero J. Pure Appl. Sci., 15 (2022) 95–104.